RSC Advances

PAPER

View Article Online
View Journal | View Issue

Cite this: *RSC Adv.*, 2017, **7**, 16662

A dual-emitting core–shell carbon dot–silica–phosphor composite for LED plant grow light†

Li Wang,[a] Haoran Zhang,[b] Xiaohua Zhou,[a] Yingliang Liu*[ab] and Bingfu Lei*[ab]

Received 6th January 2017
Accepted 27th February 2017

DOI: 10.1039/c7ra00227k

rsc.li/rsc-advances

Light-emitting diodes (LEDs) are widely used for artificial lighting in plant factories and have been applied for disease prevention and for accelerating plant growth. In this study, a unique dual-emitting core–shell CDs/$CaAlSiN_3$:Eu^{2+}-silica powder was prepared by a one-pot sol–gel method. LED devices with multi-wavelength emission (623 nm red light and 465 nm blue light) were fabricated using the as-prepared dual-emitting core–shell CDs/$CaAlSiN_3$:Eu^{2+}-silica powder, and the electrical characteristics of these LED devices were evaluated. Furthermore, it was demonstrated that these LED devices could be used for plant growth lighting in plant factories. The LEDs prepared in the present study for plant growth lighting have the advantage of being convenient, low-cost, non-toxic, and stable compared with traditional LED devices for plant growth lighting.

Introduction

The quality of the light and the carbon dioxide concentration in the environment affect the photosynthetic ability of plants.[1] In particular, the quality of the light regulates plant growth by controlling chloroplast development. In horticulture research, different artificial light sources such as metal halide lamps,[2] high-pressure sodium lamps,[3] and incandescent lamps[4] are used in various fields. However, these artificial light sources contain unnecessary wavelengths that are of low efficiency for promoting plant growth. To resolve these problems, light-emitting diodes (LEDs) are widely used for artificial lighting in plant factories and have been applied for disease prevention[5] and accelerating the plant growth. In addition, LEDs present the advantages of having an optimal efficient output and being energy-efficient,[6] thus reducing greenhouse gas emissions.[7] In recent years, researchers have proposed LED as a light source for plant growth. In principle, blue light (450–470 nm) and red light (620–630 nm and 640–660 nm) are useful for promoting photosynthesis in plants. At present, most LED plant lamps are prepared by combining blue- and red-light-emitting chips.[8] Since the two chips must be separately installed, there are lots of shortcomings such as complicated ways of sample preparation, time-consumption, and high-cost. In recent years, LED plant lamp fabricated using QDs as phosphor, and their applicability as a light source for plant growth was confirmed with multi-wavelength QD-LEDs.[9] However, semiconducting QDs contain heavy metals,[10] which pose a substantial threat and pernicious effects on the environment and human health.

On the other hand, fluorescent carbon dots (CDs) exhibit a great potential in LEDs,[11–14] sensing,[15] biosensing,[16] bioimaging,[17] and other applications due to their non-toxic nature, high biocompatibility, good chemical stability and photostability, as well as their superior optical properties.[18] CDs as blue-emitting components for multicolor luminescence can retain the chemical stability due to their strong absorption in the near-UV spectral region and efficient blue-light emission.[19,20] Moreover, $CaAlSiN_3$:Eu^{2+} phosphor has attracted significant attention for years as a red-emitting phosphor, which is essential for high-color-rendering white light-emitting diodes (LEDs) applications. Organically modified silicates and silica gels are generally excellent matrix materials, owing to their non-toxicity and inherent stability.[21] Generally, the particle size of CDs range from 8 to 9 nm, while the phosphors is very large. CD-grafted phosphors are fabricated using polymer matrix as a medium to overcome the enormous difference in size. Thus, CDs can be uniformly distributed on red-emitting phosphors to achieve different proportions of red and blue light emission.[13,14]

In this study, a unique dual-emitting core–shell CDs/$CaAlSiN_3$:Eu^{2+}-silica powder was prepared by a one-pot sol–gel method and it was used as a color converter and assembled into an UV-LED chip to construct a LED lamp for plant growth, which was less expensive and less time-consuming than the two LED chips-assembled system. Subsequently, the luminescence properties of these LED devices were systemically investigated. CDs exhibit a great potential in LED plant growth lighting due to their non-toxic nature, compared with semiconducting QDs containing heavy metals, which pose a substantial threat and harmful effects on the environment

[a]*Department of Materials Science and Engineering, College of Materials and Energy, South China Agricultural University, Guangzhou 510642, China. E-mail: tleibf@scau.edu.cn; Fax: +86 20 8528 0319; Tel: +86 20 8528 26030319*

[b]*Guangdong Provincial Engineering Technology Research Center for Optical Agriculture, Guangzhou 510642, China*

† Electronic supplementary information (ESI) available. See DOI: 10.1039/c7ra00227k

and human health. Plants grown under the LED light were significantly larger and thus more economically valuable to the farmer.

Experimental methods

Materials and reagents

Cetyltrimethyl ammonium bromide (CTAB) was purchased from Shanghai Boao Biological Technology Co. Ltd., tetraethyl orthosilicate (TEOS) was supplied from Tianjin Chemicals Co. Ltd., 1,2-bis(triethoxysilyl)ethane (BTEE) was purchased from Aladdin, and sodium salicylate (NaSal) was received from Shanghai Macklin Biochemical Co. Ltd. Ethanol (99.7%, Guangdong Guanghua Technology Co. Ltd.) and triethanolamine (TEA, ≥78.0%, Shanghai Lingfeng Co. Ltd.) were used without further purification. *N*-(β-Aminoethyl)-γ-ammonia propyl methyl dimethoxy silane (*N*-aminoethyl-3-ammonia propyl methyl dimethoxy silane) (Silane Coupler, KH-602, m.w. = 206.358) was purchased from Guangzhou Longkai Co. Ltd. and citric acid anhydrous (99.5%, AR) was purchased from Aladdin. Deionized water was used in all the experiments.

Synthesis of CDs

CDs were prepared according to a previously reported method.[22] In a typical procedure, 30 mL of Silane Coupler KH-602 was placed into a 100 mL three-necked flask and degassed with nitrogen for 10 minutes. Heat was applied until temperature reached 513 K and then 1.5 g of anhydrous citric acid was quickly added to the solution under vigorous stirring for 3 minutes. The final products were purified three times by precipitation with petroleum ether.

Preparation of CDs/$CaAlSiN_3$:Eu^{2+}-silica powder

The dual-emitting core–shell CDs/$CaAlSiN_3$:Eu^{2+}-silica powder was synthesized *via* a one-pot method using CTAB as the cationic surfactant, NaSal as the structure-directing agent, TEA as a catalyst, and BTEE and TEOS as the silica source. First, the $CaAlSiN_3$:Eu^{2+} phosphor, TEA (30 μL) and deionized water (13 mL) were added to a 100 mL round-bottom flask and then CTAB (190 mg), NaSal (84 mg), TEOS (1 mL), and BTEE (0.8 mL) were added to the above mentioned mixture. The mixture was magnetically stirred gently in an oil bath at 80 °C for 12 h. Then, CDs were added to the above mentioned and the resulting mixture was stirred for further 6 h (the $CaAlSiN_3$:Eu^{2+} phosphor to CD mass ratio was 0.06, 0.12, 0.18, 0.30, 0.50, 1.00, and 1.50). The CDs/$CaAlSiN_3$:Eu^{2+}-silica products were obtained by high-speed centrifugation and washed several times with ethanol to remove the residual reactants, followed by overnight drying in vacuum at room temperature.

Fabrication of LEDs

In a typical fabrication procedure, epoxy resin and the CDs/$CaAlSiN_3$:Eu^{2+}-silica powder were mixed by mechanical agitation, and then the mixture was integrated on the UV-LED chip (360 nm) after EDA (curing agent) was added. Finally, the LED devices for plant growth lighting were obtained after drying at room temperature for 2 h.

Characterization

Infrared spectra were obtained *via* a Fourier spectrophotometer equipped with an integrating sphere using KBr as the reference. X-ray photoelectron spectroscopy (XPS) was carried out using an AXIS ULTRA DLD, Kratos. Particle morphology was analyzed by scanning electron microscopy (SEM, XL-30; Philips, North Billerica, MA) and high resolution transmission electron microscopy (HRTEM, JEOL-2010). Photoluminescence (PL) spectra were obtained by a Hitachi F-7000 fluorescence spectrophotometer equipped with a monochromator (resolution: 0.2 nm) and a 150 W Xe lamp as the excitation source. Quantum Yield (QY) of the CDs was measured using a UV-vis spectrophotometer (UV-2550, Shimadzu). XRD patterns were obtained using powder X-ray diffraction (MSAL XD-2, China). Thermal stability tests of the material were conducted by thermogravimetric analyzer (TGA, DTG-60, Japan Shimadzu).

Results and discussion

It is well-known that light in the blue (450–470 nm) and red spectral regions (620–630 nm and 640–660 nm) are the most suitable for plant growth due to the good spectral matching with the chlorophyll absorption spectrum. In the present study, a red-emitting $CaAlSiN_3$:Eu^{2+} (623 nm) phosphor and blue-emitting CDs (465 nm) under UV excitation were selected to prepare LED grow devices, and the dual-emitting core–shell CDs/$CaAlSiN_3$:Eu^{2+}-silica powder was constructed by a one-pot sol–gel method through the hydrolysis of TEOS and BTEE (Fig. 1). There are a large amount of –COOH and –OH and other groups on the surfaces of CDs. The red-emitting phosphor

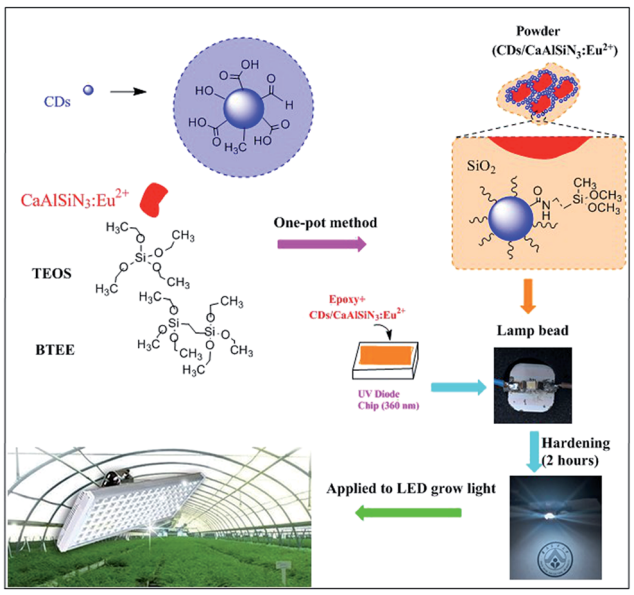

Fig. 1 Schematic for the preparation of LED grow light through a one-pot sol–gel method.

$CaAlSiN_3:Eu^{2+}$ was used as the key material for high color rendering index and low correlated color temperature solid illumination parts, which satisfies the requirements of plant grow devices.[23] However, there are no functional groups on the surface of the red phosphor $CaAlSiN_3:Eu^{2+}$. Therefore, in the present study, a strategy was presented that the CDs can be grafted onto the $CaAlSiN_3:Eu^{2+}$ phosphor surfaces through the hydrolysis and condensation reactions of TEOS and BTEE, leading to the formation of an inorganic silica and organic silica framework. The produced low polymeric hydration silicon dioxides or hydration silicon dioxides will absorb –OH on the surface of the $CaAlSiN_3:Eu^{2+}$ phosphor and start precipitating to form precipitation nuclei. A silica layer was formed by the silicon dioxide precipitate on these nuclei, and simultaneously, CDs were covalently grafted to SiO_2 by forming Si–O–Si bonds, thus accomplishing the grafting of CDs to the $CaAlSiN_3:Eu^{2+}$ phosphor. Subsequently, epoxy resin and the CDs/$CaAlSiN_3:Eu^{2+}$-silica powder could be obtained by mechanical agitation, and then the mixture was integrated on the UV-LED chip (360 nm) after EDA (curing agent) was added. Finally, the LED grow devices were obtained after drying at room temperature for 2 h.

The structures and morphology of $CaAlSiN_3:Eu^{2+}$ phosphor, CDs, and CDs/$CaAlSiN_3:Eu^{2+}$-silica powder were characterized by scanning electron microscopy (SEM) and high resolution transmission electron microscopy (HRTEM). The $CaAlSiN_3:Eu^{2+}$ phosphor was composed of well-defined plate-like primary particles, as clearly shown in Fig. 2a, and exhibited a high crystallinity with a lattice fringe distance of 0.22 nm (Fig. 2d). Fig. 2c shows the particle size of CDs in the range from 8 to 9 nm. CDs can be clearly observed throughout the formed inorganic silica and organic silica framework that coats the $CaAlSiN_3:Eu^{2+}$ phosphor surface (Fig. 2b and e), and the CDs/$CaAlSiN_3:Eu^{2+}$-silica powder exhibits a high crystallinity with a lattice fringe distance of 0.18 nm (inset of Fig. 2e). CDs are uniformly dispersed around the $CaAlSiN_3:Eu^{2+}$ phosphor to form a dual-emitting core–shell structure. This type of structure is suitable for LED grow light as it meets the requirement in plants for blue and red light.

The photoluminescence quantum yield of CDs is 29.8%, as shown in Fig. 3. To further confirm the mechanism of CDs coated with $CaAlSiN_3:Eu^{2+}$ phosphor surfaces, Fourier transformation infrared (FTIR) spectra were obtained and are shown as Fig. 4a. Several characteristic bands at around 1070 cm^{-1} (ν_{as}, Si–O), 793 cm^{-1} (ν_s, Si–O), and 450 cm^{-1} (δ, Si–O–Si) can be attributed to the vibrations of Si–O–Si. The wide vibration peak at around 3440 cm^{-1} is assigned to ν(Si–OH) and ν(O–H) in absorbed water. The vibration peaks 1515–1700 cm^{-1} could be assigned to the stretching vibration of the C=O groups from amide group (–CONR–) in CDs[15] (ν = Stretching vibration, δ = bending vibration, s = symmetric vibration, as = antisymmetric vibration). A series of XRD patterns for these samples are shown in Fig. 4b. The broad peak at about $2\theta = 23°$ indicates the amorphous phase. The XRD pattern of CDs/$CaAlSiN_3:Eu^{2+}$-silica powder agrees well with the Joint Committee on Powder Diffraction Standards (JCPDS) 39-0747, which could be ascribed to the $CaAlSiN_3:Eu^{2+}$ phosphor, as well as amorphous silica for CDs and silica. Fig. 5 shows the X-ray photoelectron spectra (XPS). The intensity of the C_{1s} peak, Si_{2p} peak and Si_{2s} peak increased for CDs-silica powder and CDs/$CaAlSiN_3:Eu^{2+}$-silica powder, relative to that of $CaAlSiN_3:Eu^{2+}$ phosphor, and it was detected by N_{1s} signal at 399 eV (C–N), showing the success of CDs-grafting on the $CaAlSiN_3:Eu^{2+}$ phosphors.[24,25] While heating up to 250 °C, the subtle weight changes of CDs/$CaAlSiN_3:Eu^{2+}$-silica powder were negligible (Fig. 4c and d). However, weight rapidly dropped when temperature increased above 250 °C. Thus, it was concluded that the CDs/$CaAlSiN_3:Eu^{2+}$-silica powder possesses an excellent thermal stability under 250 °C, indicating that this composited phosphor can be used for LED grow lamp.

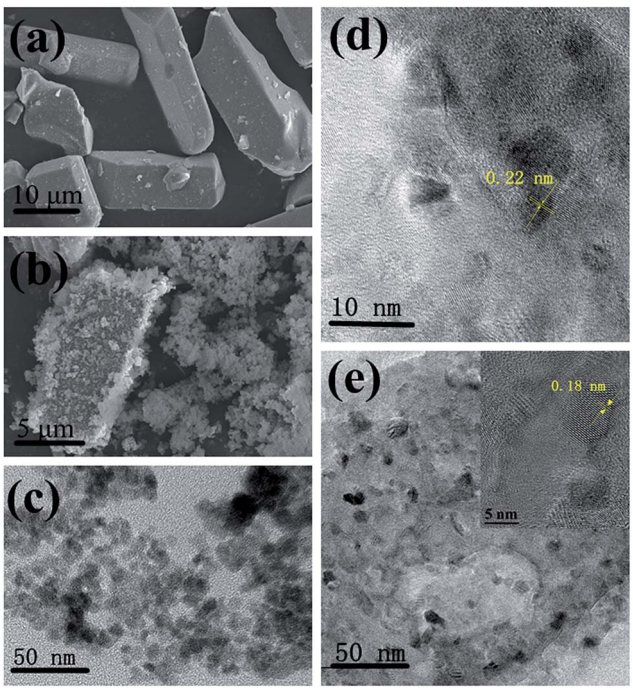

Fig. 2 SEM images of the (a) $CaAlSiN_3:Eu^{2+}$ phosphor and (b) CDs/$CaAlSiN_3:Eu^{2+}$-silica powder. HRTEM images of the (c) CDs, (d) $CaAlSiN_3:Eu^{2+}$ phosphor, and (e) CDs/$CaAlSiN_3:Eu^{2+}$-silica powder.

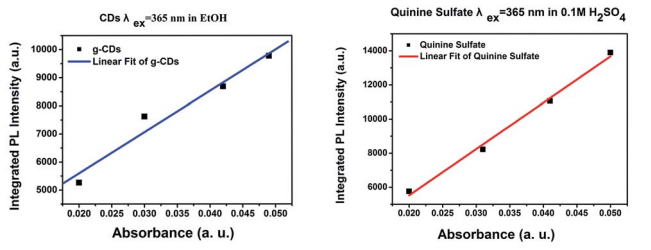

	CDs				Quinine Sulfate			
Abs	0.020	0.030	0.042	0.049	0.020	0.031	0.041	0.050
Integrated PL	5265	7621	8687	9776	5161	8225	11056	13891
Slope	1.47×10^5				2.71×10^5			
QY	29.8%				55%			

Fig. 3 Plots of the integrated PL intensity of CDs and quinolone sulfate (referenced dye) as a function of the optical absorbance at 365 nm and table with the corresponding data.

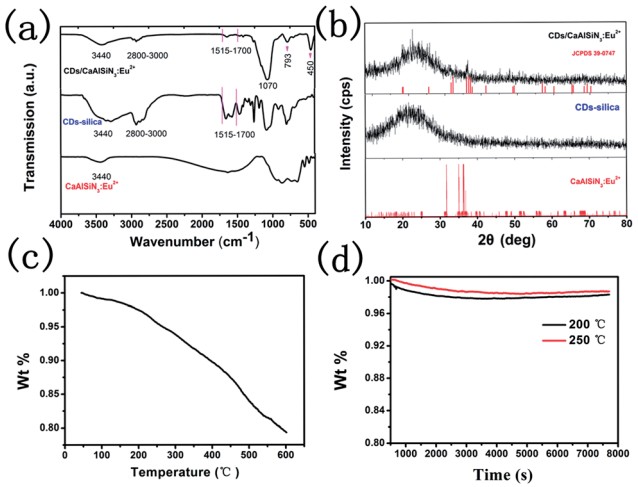

Fig. 4 (a) FTIR spectra of the $CaAlSiN_3:Eu^{2+}$ phosphor, CDs-silica powder and CDs/$CaAlSiN_3:Eu^{2+}$-silica powder. (b) XRD patterns of $CaAlSiN_3:Eu^{2+}$ phosphor, CDs-silica powder and CDs/$CaAlSiN_3:Eu^{2+}$-silica powder. The standard data for the $CaAlSiN_3:Eu^{2+}$ phosphor (JCPDS card no. 39-0747) is shown as a reference. (c) TGA of the CDs/$CaAlSiN_3:Eu^{2+}$-silica powder. (d) TGA of the CDs/$CaAlSiN_3:Eu^{2+}$-silica powder at 200 °C and 250 °C.

$CaAlSiN_3:Eu^{2+}$ phosphor shows a broad excitation band which is suitable for the conversion of both CDs and near-ultraviolet[26] (Fig. 6a). The $CaAlSiN_3:Eu^{2+}$ phosphor exhibits a highly saturated deep red emission with a dominant wavelength of 623 nm and corresponding chromaticity coordinates of (0.63, 0.37). CDs exhibited an emission band at 465 nm under 394 nm excitation (Fig. 6b) and corresponding chromaticity coordinates of (0.17, 0.13). Fig. 6d shows the normalized fluorescence spectra of the $CaAlSiN_3:Eu^{2+}$ phosphor, CDs, and CDs/$CaAlSiN_3:Eu^{2+}$-silica powder (mass ratio: 1.00). As expected, CDs/$CaAlSiN_3:Eu^{2+}$-silica powder displays both characteristic emissions of the $CaAlSiN_3:Eu^{2+}$ phosphor and CDs under 362 nm excitation (Fig. 6c). However, the characteristic emission of CDs was blue-shifted relative to that of the free state of

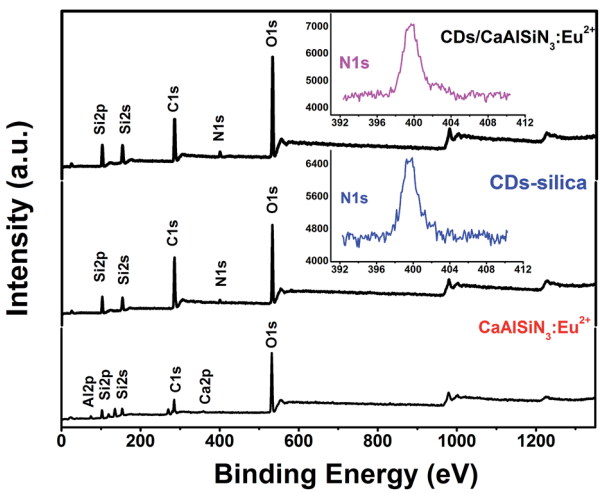

Fig. 5 XPS of the $CaAlSiN_3:Eu^{2+}$ phosphor, CDs-silica powder, and CDs/$CaAlSiN_3:Eu^{2+}$-silica powder.

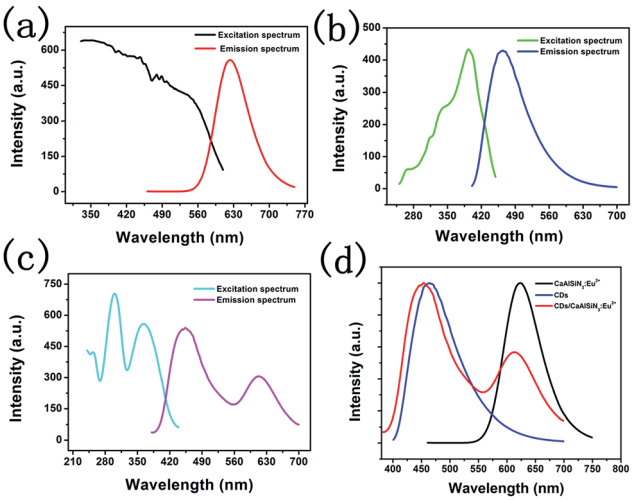

Fig. 6 (a) Excitation and emission spectra of the $CaAlSiN_3:Eu^{2+}$ phosphor (excited at 450 nm), (b) excitation and emission spectra of CDs (excited at 394 nm), (c) excitation and emission spectra of CDs/$CaAlSiN_3:Eu^{2+}$-silica powder (mass ratio: 1.00) (excited at 362 nm), and (d) normalized fluorescence spectra of the $CaAlSiN_3:Eu^{2+}$ phosphor, CDs and CDs/$CaAlSiN_3:Eu^{2+}$-silica powder (mass ratio: 1.00).

CDs, which might be due to the luminous performance of CDs being affected by the surrounding environment and surface state. This would mean that the phenomenon was due to the change of surface state of CDs coating with $CaAlSiN_3:Eu^{2+}$ phosphor.[27] It was also observed from Fig. 7a and b that under 400 nm excitation wavelength, the strongest emission of CDs peak position is 465 nm relative to the 460 nm of CDs/$CaAlSiN_3:Eu^{2+}$-silica powder. Specifically, the excitation wavelength-dependence of the free state of CDs could be

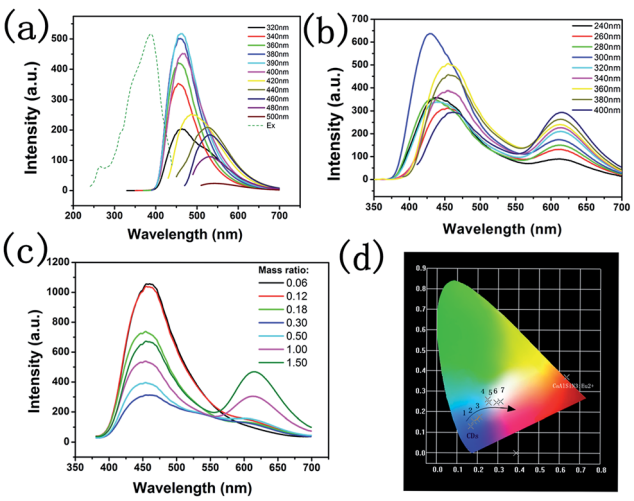

Fig. 7 (a) Fluorescence spectra of a CDs solution excited at different excitation wavelengths and excitation spectrum of CDs monitored at 465 nm. (b) Emission spectra of CDs/$CaAlSiN_3:Eu^{2+}$-silica powder (mass ratio: 1.00) excited at different wavelengths from 240 to 400 nm. (c) Emission spectra and (d) CIE chromaticity diagram for CDs/$CaAlSiN_3:Eu^{2+}$-silica powder with different mass ratios: 0.06, 0.12, 0.18, 0.30, 0.50, 1.00, and 1.50. All samples were excited at 362 nm.

represented as the excitation wavelength change from 340 nm to 500 nm, corresponding to the peak position of CDs ranging from 454 nm to 543 nm, which suggests that CDs is red-shifted. Similarly, the excitation wavelength of CDs/$CaAlSiN_3$:Eu^{2+}-silica powder changed from 280 nm to 400 nm, corresponding to the characteristic peak position of CDs ranging from 428 nm to 555 nm. This difference can be attributed to the lowered excitation energy, leaving various higher emission energy levels inaccessible and increasing the associated energy for the Stokes shift in each case.[14,28] As there are obvious differences in the emission bands with different mass ratios, we could easily tune the emission wavelength of the CDs by adjusting the mass ratio, which led to more relative emission intensities of the CDs/$CaAlSiN_3$:Eu^{2+}-silica powder. The additive primaries CDs and $CaAlSiN_3$:Eu^{2+} phosphor can be mixed in different red-blue light proportions to meet the light quality needed for plant growth, germination, blooming, and seed setting. As shown in Fig. 7c, the characteristic emission intensity of both CDs and $CaAlSiN_3$:Eu^{2+} phosphor systematically changed with different mass ratios. The results indicated that, as the mass ratio increased, the characteristic emission intensity of CDs decreased and then increased, whereas the characteristic emission intensity of the $CaAlSiN_3$:Eu^{2+} phosphor steadily increased. In accordance with the CIE chromaticity coordinates shown in Fig. 7d, the samples numbered from 1 to 7 correspond to different relative concentrations of $CaAlSiN_3$:Eu^{2+}/CDs (mass ratio: 0.06, 0.12, 0.18, 0.30, 0.50, 1.00, and 1.50, respectively) and the color footprints numbered from 1 to 7 ran across the (0.183, 0.154), (0.197, 0.166), (0.211, 0.174), (0.249, 0.259), (0.256, 0.245), (0.293, 0.244) and (0.313, 0.251) coordinates, respectively.

As shown in Fig. 8a, the luminescence intensity of CDs gradually decreased with the increasing concentration of $CaAlSiN_3$:Eu^{2+}, whereas the characteristic luminescence intensity of $CaAlSiN_3$:Eu^{2+} phosphor was strengthened. Moreover, when using the LED lamp, the luminescence intensity regularly changed as compared with that of the emission spectra of the powders (Fig. 7c). The corresponding CIE chromaticity diagram of the samples under 362 nm excitation is shown in Fig. 8b. The color footprints ran across the (0.230, 0.227), (0.294, 0.280), (0.356, 0.343), (0.388, 0.422), (0.462, 0.415), (0.493, 0.390) and (0.583, 0.409) coordinates. The additive primaries CDs and $CaAlSiN_3$:Eu^{2+} phosphor can be mixed in different proportions to prepare a LED device for plant growth with the required red-blue proportion. It is important to select artificial lighting that provides both ends of the spectrum in sufficient intensity to cater for different plant needs. Fig. 8c shows the electroluminescence spectra of the LED device at an optimized current of 20 mA with two emission bands: one characteristic band at 470 nm and another at 612 nm. The opposite intensity of the two characteristic bands led to a white-light with the corresponding CIE coordinates of (0.294, 0.280) and (0.356, 0.343), which are very close to those of the ideal white light (0.333, 0.333). Interestingly, the white-light LED exhibited a high color rendering index (CRI) of 85 and 86, which is much higher than that of the YAG:Ce-based commercial white LED (CRI 75).[29]

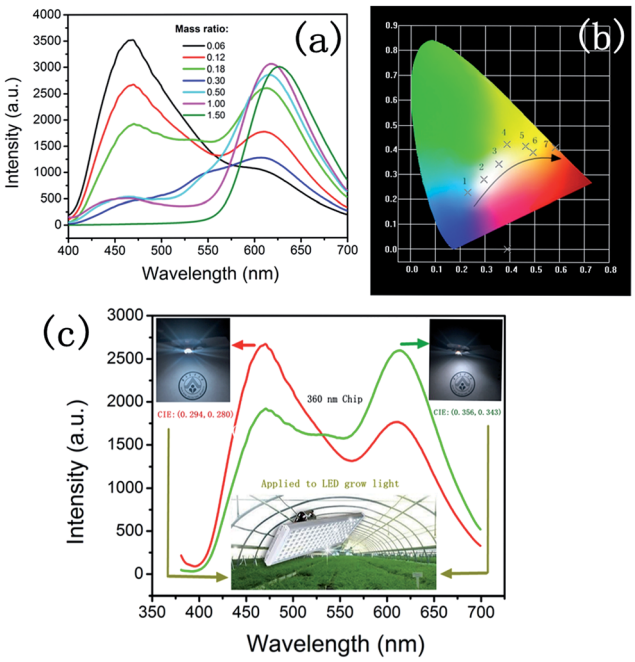

Fig. 8 (a) Emission spectra of the LED lamp fabricated with $CaAlSiN_3$:Eu^{2+}/CDs with different mass ratios: 0.06, 0.12, 0.18, 0.30, 0.50, 1.00, and 1.50. All samples were excited at 362 nm; (b) CIE chromaticity diagram for the LED lamp fabricated with $CaAlSiN_3$:Eu^{2+}/CDs with different mass ratios: 0.06, 0.12, 0.18, 0.30, 0.50, 1.00, and 1.50. All samples were excited at 362 nm; and (c) electroluminescence spectra of the LED lamp fabricated using a 360 nm chip combined with a white-emitting $CaAlSiN_3$:Eu^{2+}/CDs (mass ratio: 0.12 and 0.18).

To evaluate the possibility of using these LED devices for plant growth lighting in plant factories, parallel experiments were performed using the as-prepared LED grow devices and the commercial white LED lamp as a control group to cultivate lettuce and garland chrysanthemum, as shown in Fig. S1 (ESI, d(1–3) and f(1–3)†). After 21 days, the results of the experiments indicated that the average output of the experimental group (R/B 3.515) was better than that of the control group (white LED), and the average output in the experimental group (R/B 0.637) was more abundant than that in the control group (white LED). Red light promoted the radial growth of lettuce and garland chrysanthemum plants, and blue light was beneficial for transverse extension. Lettuce could not normally grow under pure red light, and with the gradual increase of blue light proportion (5–20%), there were some effects on the growth of lettuce; for instance, the improvement of photosynthesis, increased content of carotenoids, chlorophyll, and nutrients, and the increase of the total biomass. As a result, the growth and physiological characteristics of lettuce and garland chrysanthemum plants were evaluated, and results were used to select the best combination of red and blue LED for plant growth.

Conclusions

In this study, LED grow devices were fabricated using dual-emitting CDs/$CaAlSiN_3$:Eu^{2+}-silica powder, and its applicability as a lighting source for plant growth with multi-

wavelength emission (red and blue light wavelength) was demonstrated. The as-obtained CDs/$CaAlSiN_3$:Eu^{2+}-silica powder has a core–shell structure and was obtained by a one-pot sol–gel method through the hydrolysis of TEOS and BTEE. As a result, an improved LED grow devices could be achieved by combining the as-prepared blue-emitting CDs and red-emitting $CaAlSiN_3$:Eu^{2+} phosphor as color converters in a UV-LED chip. The LED grow devices are less costly and less time-consuming than the traditional two LED chips assembled system. On the other hand, our as-prepared LED device is convenient, low-cost, non-toxic, and inherently stable compared to traditional LED devices. Additionally, the combination of red and blue light in our LED device promotes plant growth, with the red light promoting radial growth of plants, and the blue light favoring transverse extension.

Acknowledgements

The present work was supported by the National Natural Science Foundation of China (Grant No. 21671070, 21571067), the Teamwork Projects funded by the Guangdong Natural Science Foundation (Grant No. S2013030012842), the Project for Construction of the High-level University in the Guangdong Province, the Provincial Science and Technology Project of the Guangdong Province (No. 2014A010105035, 2016A050502043, 2015B090903074), and the Guangzhou Science & Technology Project (No. 201605120833193, 201605030005).

References

1 K. Fujiwara, T. Kozai and I. Watanabe, *J. Agric. Meteorol.*, 1987, **43**, 21–30.
2 H. I. Lee, Y. H. Kim and D. E. Kim, *J. Biosyst. Eng.*, 2010, **35**, 413–419.
3 W. C. Randall and R. G. Lopez, *HortScience*, 2014, **49**, 589–595.
4 F. Kohyama, C. Whitman and E. S. Runkle, *HortTechnology*, 2014, **24**, 490–495.
5 C. A. Metildi, C. S. Snyder and M. Bouvet, *J. Am. Coll. Surg.*, 2012, **214**, 997–1007.
6 T. T. Member, *IEEJ Trans. Electr. Electron. Eng.*, 2007, **3**, 21–26.
7 D. Singh, C. Basu, M. M. Wollweber and B. Roth, *Renewable Sustainable Energy Rev.*, 2015, **49**, 139–147.
8 J. Lei, N. Zhang, R. Yan, L. X. Xu, Y. Li and W. Q. Guan, *Trans. Chin. Soc. Agric. Eng.*, 2016, **32**, 248–254.
9 J. W. Song, *Journal of International Council on Electrical Engineering*, 2016, **6**, 13–16.
10 J. B. Xiao, Y. Bai, Y. F. Wang, J. W. Chen and X. L. Wei, *Spectrochim. Acta, Part A*, 2010, **76**, 93–97.
11 F. Wang, Y. H. Chen, C. Y. Liu and D. G. Ma, *Chem. Commun.*, 2011, **47**, 3502–3504.
12 X. Guo, C. F. Wang, Z. Y. Yu, L. Chen and S. Chen, *Chem. Commun.*, 2012, **48**, 2692–2694.
13 Y. H. Chen, B. F. Lei, M. T. Zheng, H. R. Zhang, J. L. Zhuang and Y. L. Liu, *Nanoscale*, 2015, **7**, 20142–20148.
14 W. Li, H. R. Zhang, S. Chen, Y. L. Liu, J. L. Zhuang and B. F. Lei, *Adv. Opt. Mater.*, 2016, **4**, 427–434.
15 B. F. Lei, L. Wang, H. R. Zhang, Y. L. Liu, H. W. Dong, M. T. Zheng and X. H. Zhou, *Sens. Actuators, B*, 2016, **10**, 101–108.
16 B. Wang, Y. F. Chen, Y. Y. Wu, B. Weng, Y. S. Liu, Z. S. Lu, C. M. Li and C. Yu, *Biosens. Bioelectron.*, 2016, **78**, 23–30.
17 L. Wang, Y. Yin, A. Jain and H. Susan Zhou, *Langmuir*, 2014, **30**, 14270–14275.
18 S. Zhu, Y. Song, X. Zhao, J. Shao, J. Zhang and B. Yang, *Nano Res.*, 2015, **8**, 355–381.
19 S. S. Babu, M. J. Hollamby, J. Aimi, H. Ozawa, A. Saeki, S. Seki, K. Kobayashi, K. Hagiwara, M. Yoshizawa and H. Möhwald, *Nat. Commun.*, 2013, **4**, 1969, DOI: 10.1038/ncomms2969.
20 Y. Wang, R. Hu, G. Lin, I. Roy and K. Yong, *ACS Appl. Mater. Interfaces*, 2013, **5**, 2786–2799.
21 Q. Chen, C. Wang and S. Chen, *J. Mater. Sci.*, 2013, **48**, 2352–2357.
22 F. Wang, Z. Xie, H. Zhang, C. Y. Liu and Y. G. Zhang, *Adv. Funct. Mater.*, 2011, **21**, 1027–1031.
23 S. X. Li, X. Peng, X. J. Liu and Z. R. Huang, *Opt. Mater.*, 2014, **38**, 242–247.
24 L. Sun, C. Tian, Y. Fu, Y. Yang, J. Yin, L. Wang and H. Fu, *Chem.–Eur. J.*, 2014, **20**, 564–574.
25 Y. H. Chen, M. T. Zheng, Y. Xiao, H. W. Dong, H. R. Zhang, J. L. Zhuang, H. Hu, B. F. Lei and Y. L. Liu, *Adv. Mater.*, 2016, **28**, 312–318.
26 K. Uheda, N. Hirosaki, Y. Yamamoto, A. Naito, T. Nakajima and H. Yamamoto, *Electrochem. Solid-State Lett.*, 2006, **9**, 22–25.
27 A. Rogach, A. Susha, F. Caruso, G. Sukhorukov, A. Kornowski, S. Kershaw, H. Mohwald, A. Eychmiiller and H. Weller, *Adv. Mater.*, 2000, **12**, 333–337.
28 Y. Wang, S. Kalytchuk, Y. Zhang, H. Shi, S. V. Kershaw and A. L. Rogach, *J. Phys. Chem. Lett.*, 2014, **5**, 1412–1420.
29 K. Park, T. Kim, Y. Yu, K. Seo and J. Kim, *J. Lumin.*, 2016, **173**, 159–164.